Nonlocal electromagnetic generation and detection of ultrasound in potassium*

D. E. Chimenti, Carl A. Kukkonen, and B. W. Maxfield
Laboratory of Atomic and Solid State Physics
and The Materials Science Center, Cornell University, Ithaca, New York 14850
(Received 15 April 1974)

The amplitude of electromagnetic generation of ultrasound in single-crystal potassium has been measured at $T = 4.2$ K as a function of magnetic field from 0 to 15 kG at a frequency of 8.97 MHz, using inductive means for *both* generation and detection of the acoustic wave. At zero magnetic field the measured amplitude is several times larger than the predicted free-electron value, and between 0 and 3 kG the experimental curve is well outside the predicted behavior. From 9 to 14 MHz the frequency dependence of the measured amplitude exhibits the expected behavior. An attempt has been made to rework the theory in the usual approximations to explain the discrepancy observed. It is shown that no simple modification of free-electron theory can account for the measured enhancement of the zero-field electromagnetic-generation amplitude. The experimental results are discussed in the light of previous measurements in potassium.

I. INTRODUCTION

Electromagnetic generation of ultrasound in metals[1,2] has been investigated experimentally and theoretically for several years. When a radio-frequency electromagnetic wave impinges on the surface of a metal in the presence of a large static magnetic field normal to the surface, the Lorentz force on the induced electron current in the skin depth adds to the Lorentz force on the lattice ions, giving rise to an acoustic shear wave which propagates away from the surface with its polarization perpendicular to the rf electric field. At zero magnetic field the conduction electrons are accelerated in one direction by the rf electric field, the lattice ions in the other. The relevant parameters here are the electron mean free path l and the skin depth δ. In the local limit, $l \ll \delta$, the electrons collide with the lattice on a scale that is small compared to the variation of the rf fields in the metal. Thus the electron reaction force microscopically cancels the ion momentum, leaving a zero net shear force on the lattice. However, if $l \gtrsim \delta$ (the nonlocal limit), electrons travel farther than the skin depth into the metal before scattering, leaving uncanceled ion momentum in the skin-depth region which produces a net ion displacement, that is, an acoustic shear wave. The exact acoustic amplitude as discussed in Sec. II is a complicated function of the product of l and the acoustic wave vector q, as well as other parameters.

Early work on this effect centered on experimentally convenient metals like Al, Ag, and W.[3-5] Later, when quantitative comparisons with existing theory based on free-electron assumptions[6] were desired, interest in metals having a simple band structure increased.

Existing experimental results on potassium are inconclusive. While the measurements of Turner, Thomas, and Hsu[7] (TTH) seem to be in agreement with the free-electron calculations of Quinn,[6] certain aspects of their experiment are problematic. For one, while a rf field is used to generate the acoustic wave, detection is accomplished by a piezoelectric transducer bonded to the potassium sample. Normally, this would not be an objectionable procedure, but owing to the soft and highly reactive nature of the metal, it is possible that an imperfect bond or a highly strained sample might affect the results. More important, however, is the fact that the acoustic attenuation of the potassium sample was determined by attaching a second transducer. This method almost certainly strains the surface. Although the surface was etched before each electromagnetic-generation measurement, it is possible that some surface damage remained and that the electronic mean free path near the surface could be different from the bulk.

Wallace, Gaerttner, and Maxfield[8] (WGM) have done similar measurements; however, they measure the acoustic attenuation of their sample in a manner consistent with the preservation of one surface of low strain. As in the TTH experiment a transducer is used for detection of the acoustic wave. In contrast with the results of TTH, the data of WGM at low magnetic field show an anomalous behavior not predicted by theory.[6] Also, the magnitude of the zero-field generation is found to be several times larger than predicted by free-electron theory.

We have measured the conversion efficiency for this electromagnetic-generation (EG) process, which is proportional to the lattice wave amplitude squared, utilizing inductive means for *both* generation and detection of the acoustic wave. Our measurement seeks to relieve some of the ambiguity of the previous experiments by eliminating the piezoelectric transducer altogether. To ac-

complish this, a considerable improvement in sensitivity is required since the zero-field EG amplitude at 10 MHz is about 40 db below the acoustic signal level of an average quartz transducer. The two principal developments which have been instrumental in the success of the present experiment are improved sample preparation and multichannel signal averaging. The measurements have been performed on a strain-free single-crystal potassium specimen as a function of applied magnetic field from 0 to 15 kG at a temperature of 4.2 K. Because of the nature of the data, detailed comparison with previous work is not straightforward, as will be shown later. However, some definite conclusions can be drawn. These are summarized graphically in Fig. 1. Here, we plot the measured electromagnetic-generation amplitude versus magnetic field from 0 to 4 kG. The shaded area in Fig. 1 represents the limits of the free-electron theory prediction for values of the electron mean free path, the only adjustable parameter, both large and small compared to the acoustic wavelength. We find that (i) at zero magnetic field the measured amplitude is several times larger than the free-electron value, in qualitative agreement with WGM and in clear disagreement with TTH; (ii) between 0 and 3 kG the experimental curve is well outside the predicted behavior, which tends to support the observations of WGM, while direct comparison with TTH in this field region is difficult; (iii) the only adjustable parameter in the well-established free-electron theory is the electron mean free path, and from Fig. 1 it is apparent that no value of l will provide agreement with the data at zero field; (iv) there is no simple way to modify the free-electron theory to account for the measured discrepancy.

In Sec. II the theory of electromagnetic generation is presented. Section III deals with experimental technique, and Sec. IV contains a description of the data analysis. Results and discussion are presented in Sec. V.

II. THEORY

The free-electron theory for the electromagnetic generation of acoustic shear waves is well established.[6,9-11] The basic ideas can be characterized in the following way. In the long-wavelength limit one treats the lattice as a uniform elastic medium which is described by the standard wave equation. The forces acting on the lattice are due to the electric field within the skin depth, the Lorentz force of the external magnetic field B, and the reaction force due to electrons colliding with the lattice. The equation of motion for the lattice is

$$M\frac{\partial^2\vec{\xi}}{\partial t^2} - C\frac{\partial^2\vec{\xi}}{\partial z^2} = e\left(\vec{E} + \frac{1}{c}\frac{\partial\vec{\xi}}{\partial t}\times\vec{B}\right) + \vec{F}_r\,,$$
$$F_r = \frac{-e}{\sigma_0}\left(\vec{J}_e + ne\frac{\partial\vec{\xi}}{\partial t}\right), \tag{1}$$

where $\vec{\xi}$ is the lattice displacement, M the ion mass, C the elastic constant, $\vec{E}$ the electric field in the metal, F_r the electron reaction force, σ_0 the dc conductivity, n the carrier density, e the electron charge, and c the speed of light. The electron current $\vec{J}_e$ is obtained from the Boltzmann equation (in the relaxation-time approximation) in terms of

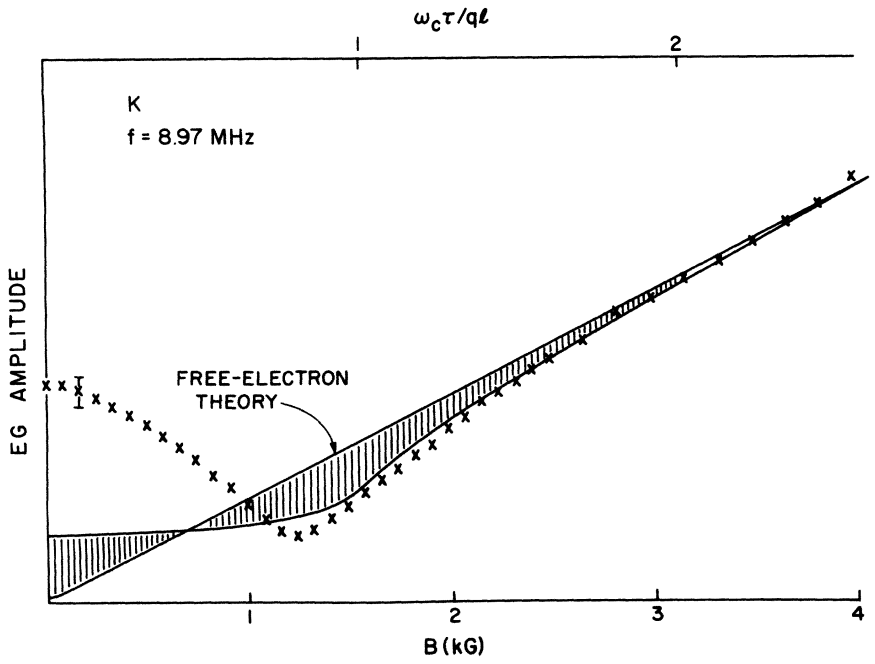

FIG. 1. Electromagnetic generation amplitude vs magnetic field at $T = 4.2$ K. Vertical scale is in relative units. Shaded region shows the limits of free-electron prediction with upper curve at zero field representing larger mean free path. Experimental uncertainty in low-field region is indicated by a typical error bar.

$\vec{E}$ and $\partial\vec{\xi}/\partial t$.[10,11] Maxwell's equations relate the electric field to the total current. This then allows one to solve for $\vec{\xi}$. It is assumed that the lattice ions form a free surface with $\partial\vec{\xi}/\partial z = 0$ at $z = 0$, and that the electrons are specularly scattered from the surface, that is, the electron velocities before and after reflection are related by $V_x' = V_x$, $V_y' = V_y$, $V_z' = -V_z$. Quinn[6] has given the Fourier transform of the circularly polarized components of the ion displacement. Gaerttner[8,9] and TTH have approximately performed the Fourier transform to obtain the real-space ion amplitude at the generating surface in the limit $q\delta$ and $\omega\tau \ll 1$, where $q = \omega/s$ is the acoustic wave vector, ω is the angular frequency, τ is the electron relaxation time, and s is the velocity of sound. Solving Eq. (1) one finds

$$\vec{\xi}(z=0) = A(\omega\tau)^{-1}\{\hat{x}[(1-G_+^{-1})+(1-G_-^{-1})] - i\hat{y}[(1-G_+^{-1})-(1-G_-^{-1})]\}, \quad (2)$$

where $A = icmh_0/8\pi\rho se$, h_0 is the excitation magnetic field along $\hat{y}$, ρ the mass density, and m the electron mass. The function $G_\pm$, which is explicitly given in Refs. 9 and 11, is related to elements of the magnetoconductivity tensor $\overleftrightarrow{\sigma}$ by $G_\pm = \sigma_0^{-1}(\sigma_{xx} \pm \sigma_{xy})$. $G_\pm$ is a function of the frequency, the external magnetic field, and the electron mean free path $l = v_F\tau$, where v_F is the Fermi velocity.

In zero external magnetic field, $G_+ = G_-$ is a real quantity given by

$$G_+ = \frac{3}{2(ql)^2}\left(\frac{1+(ql)^2}{ql}\arctan(ql) - 1\right). \quad (3)$$

Thus $\vec{\xi}$ has only an x component which is sometimes referred to as the nonmagnetic component, designated $\vec{\xi}_E$. In the high-field limit, $\omega_c\tau \gg ql$, or equivalently, $\omega_c \gg qv_F$,

$$G_\pm^{-1} \cong 1 \pm i\omega_c\tau, \quad (4)$$

where $\omega_c = eB/mc$ is the electron cyclotron frequency. In this limit $\vec{\xi}$ has only a y polarization which is called the magnetic component and is given by

$$\vec{\xi}_H = 2A\omega_c\omega^{-1}\hat{y}. \quad (5)$$

Note that $\vec{\xi}_H$ is independent of the electron mean free path.

As long as $\omega\tau \ll 1$, $G_+ \approx G_-^*$ and Eq. (2) can be written as

$$\vec{\xi}(z=0) = 2A(\omega\tau)^{-1}[\hat{x}\,\mathrm{Re}(1-G_+^{-1}) + \hat{y}\,\mathrm{Im}(1-G_+^{-1})]. \quad (6)$$

Now one can see from Eq. (6) that the x and y components of $\vec{\xi}$ are in phase. A more detailed discussion of this result is presented in Sec. IV.

To compare theory and experiment, one measures the high-field amplitude and fits it to Eq. (5) to determine the constant A. The electron mean free path l can be estimated from the electrical resistivity or the magnetic field dependence of the ultrasonic attenuation. Once the values of A and l are determined, one has completely specified both components of the acoustic wave amplitude.

III. EXPERIMENTAL TECHNIQUE

In this experiment we utilize the conventional geometry, depicted in Fig. 2. Small, flat spiral coils wound from No. 40 copper wire and potted in clear epoxy are mounted within about 0.25 mm of the sample surface. Each coil, about 1 cm in diameter, has 40–50 turns and is held accurately concentric in a brass iris to prevent field distortion. The 24-mm-wide irises slide smoothly on stainless-steel rods to allow for mounting and dismounting of samples. A more complete description of a similar apparatus is given elsewhere.[12] Electrical connection is made to the coils by means of a silver-plated, stainless-steel coaxial transmission line with Teflon dielectric.

The specimen upon which all measurements have been performed has been carefully string cut from a large single-crystal boule of high-purity potassium.[13] Grown by a standard Bridgman technique, the boule has been oriented to within 1° by a x-ray transmission method. The [100] axis is perpendicular to the plane of the sample and parallel to the direction of propagation of the sound wave and the magnetic field. Preparation of the surfaces is accomplished by the use of a fairly sophisticated crystal-facing instrument which is composed of a 25-cm vertically mounted stainless-steel lapping wheel across which high-grade wool cloth is stretched. The cloth is soaked with etchant, and the sample is suspended against the wheel in such a way that only the meniscus of the fluid makes contact with the surface being polished. In this way a very smooth surface whose electrical properties are probably representative of the bulk can be prepared. Residual resistance ratios of samples from the same boule are typically 3000–3500. But since the sample used in this measurement was cooled slowly to 273 K before quenching to 77 K, its resistance ratio is estimated to be about 4500.[14] The specimen preparation procedure is described in full detail in Ref. 12.

Figure 3 shows the usual instrumentation used in this type of experiment. Radio-frequency pulses about 1 μsec in duration (250-W peak power) are sent to the drive coil through an impedance matching network. Occasionally, a 3- or 6-dB attenuator is inserted between the matching network and the drive coil to reduce ringing when the pulse generator turns off. On the pickup side another matching network, adjusted for maximum signal, precedes a typical superheterodyne receiver. Af-

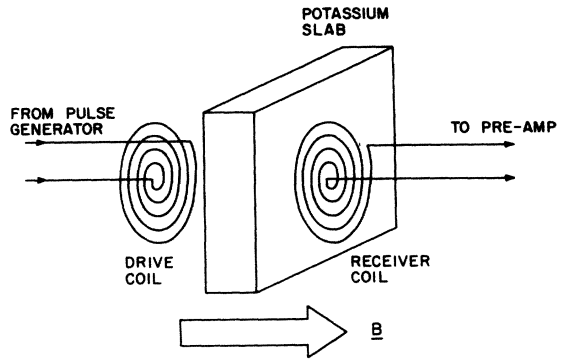

FIG. 2. Sample geometry of electromagnetic generation experiment. Coils are placed 0.25 mm from sample surface.

ter 40 or 60 dB of preamplification, the signal is mixed with the local oscillator frequency to produce a 32-MHz if signal. About 90 dB of if gain precedes diode detection; then the signal is displayed on an oscilloscope. If an attenuation measurement is being made, the echo decay pattern also goes to a 1000-channel transient recorder, the memory of which is strobed at a rate of 50 Hz into a signal averager, thus accumulating an integrated representation of the signal. When a field-dependence measurement is performed, the detected signal is sent to a gated integrating amplifier whose aperture width of 200 nsec is centered on the second echo (three passes through the sample). The magnetic field is then swept slowly at a rate of 7 G/sec to minimize problems of response time, while the amplifier output and magnetic field are simultaneously recorded. Typical signals after 16 000 averages show seven or eight discernible echoes at zero magnetic field. In the low-field region between 1 and 2 kG, as few as three echoes are sometimes usable because of the reduction in generation amplitude.

A very important aspect of these measurements is the calibration of the electronics. The calibration system is represented in Fig. 3 enclosed in dashed lines. It consists of a cw oscillator, tuned to the experimental frequency, whose output is fed to one port of a rf mixer. The other port receives a 1-μsec pulse from the pulse generator. This arrangement yields clean, sharp pulses with on/off ratios of greater than 40 dB. Completing the system is a calibrated attenuator whose impedance is well matched to the mixer and the preamplifier.

The experimental frequency is determined by mixing the pulse electronically with the output of a stable cw oscillator whose frequency is monitored by a digital electronic counter. When the mixer output displays a characteristic zero-beat pattern, the frequency is given to ± 10 kHz by the electronic counter. A 15-kG superconducting solenoid supplies the static magnetic field for these measurements. The magnet has been calibrated at several field values by proton NMR.

IV. DATA ANALYSIS

In analyzing and drawing conclusions from the data obtained in this experiment several factors are of particular importance. First, let us consider the geometry of the coils that are used to generate and detect the acoustic wave. They are of the flat spiral design as shown in Fig. 2 and couple to an acoustic shear wave whose polarization is a function of azimuthal angle about the center of the coil. Keep in mind that the sample normal is accurately parallel to a [100] crystal axis, so that the two shear velocities are degenerate. Since the coils are 12 mm in diameter, beam spread at the fourth echo is only about 4%. Therefore, the sound wave produced by each differential area of the drive coil propagates to an identical area on the receiver coil with minimal beam spread over the distance of interest.

One possible complication to be noted is the existence of magnetoacoustic rotation of the polarization direction of a plane-polarized sound wave, which has been predicted by Kjeldaas.[11] However, the maximum error, which occurs in the vicinity of $\omega_c \tau/ql = 1$, introduced by ignoring this effect is about 7% at the fourth echo. At the position of the second echo, the one monitored in measuring the magnetic field dependence of EG, the error is under 2%. At magnetic fields such that $\omega_c \tau/ql \gg 1$ or $\ll 1$, the magnetoacoustic rotation is negligible. Since echoes beyond the fourth are not used in determining attenuation in the critical region, the systematic errors introduced by ignoring this effect are well below other sources of uncertainty.

Perhaps the major uncertainty in the experimental curve arises in the determination of the

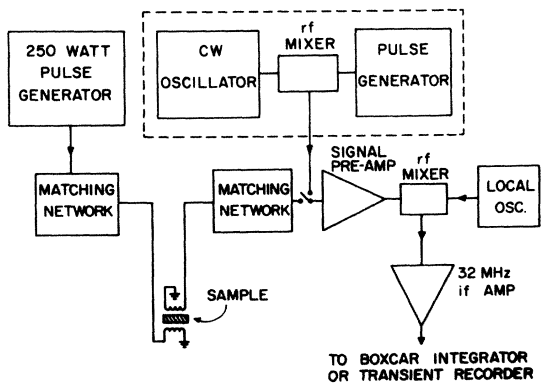

FIG. 3. Experimental instrumentation for pulse-echo measurements.

acoustic attenuation as a function of magnetic field. The electronic component of the acoustic attenuation is separated from the total attenuation by assuming that at high magnetic field, $\omega_c\tau \gg ql$, the electronic contribution is zero, as predicted by Kjeldaas.[11] While very careful and meticulously calibrated measurements of the echo decay pattern were made at field intervals of about 200 G throughout the critical region where the attenuation changes rapidly with field, errors in determining the total attenuation are estimated at about 10 or 15%. This rather large uncertainty is due partly to extremely small signals at some fields, and partly to the somewhat nonexponential character of the echo decay envelope. In fact, an attempt to determine ql by fitting the Kjeldaas theory to our attenuation data has been largely unsuccessful owing in part to the large error bars. Instead we have relied on the mean-free-path estimate from resistance ratio measurements to infer ql; we obtain a value between 4 and 5 at 9 MHz. Blaney[15] has noted behavior in the magnetic field dependence of the shear-wave attenuation in potassium at 50 MHz which is rather similar to our own findings. It should also be mentioned that we find the electronic component of the ultrasonic attenuation to be about two times larger than the free-electron prediction of Pippard.[16] In the local regime ($ql \ll 1$) Natale and Rudnick[17] have observed similar enhancements in the electronic attenuation of longitudinal waves in potassium. While surface nonparallelism is a possible explanation of our results, we were led to perform some additional measurements. To verify the accuracy and reliability of our method, the electronic component of the acoustic attenuation in high-purity aluminum has been measured at zero magnetic field using a quartz transducer for generation and a double-spiral coil, which is sensitive to the polarized acoustic wave from the transducer, for detection. The resulting value at 11.26 MHz is about 9 dB/cm, within 20% of the free-electron prediction.

To determine just what it is that the coils are measuring we must now investigate the phase of $\vec{\xi}_H$ and $\vec{\xi}_E$. From Eq. (6), one can see that in the limit $q\delta \ll 1$, $\omega\tau \ll 1$, the phases of the two polarizations are nearly equal. As the magnetic field is increased beyond $\omega_c\tau/ql = 1$, the phase of $\vec{\xi}_E$ changes relative to $\vec{\xi}_H$. But by the time $\cos\phi_{E,H} = 0.99$, where $\phi_{E,H}$ is the phase difference, the contribution of $\vec{\xi}_E$ to the total signal is negligible (2%). This fact has also been verified numerically for somewhat more general conditions. Because the magnetic and nonmagnetic signals are very nearly in phase and represent orthogonal ion displacements, we infer that, apart from the nearly negligible magnetoacoustic rotation, the receiver-coil voltage V_{expt} is given by

$$V_{\text{expt}} \propto \omega^2(|\vec{\xi}_E|^2 + |\vec{\xi}_H|^2). \tag{7}$$

Thus the induced voltage in the receiver coil is a square sum of the two components which could be determined independently in a measurement utilizing a quartz transducer for either detection or generation of the acoustic signal. However, in a two-coil experiment with the sound wave propagating along a symmetry direction where the shear velocities are degenerate, a geometry which would allow the separate measurement of $\vec{\xi}_E$ and $\vec{\xi}_H$ is impossible to construct. Even the use of coils that generate acoustic waves of well-defined polarization would not suffice.

The problem lies in the symmetric nature of the generation and detection process. Consider two polarized coils at opposite ends of a metal specimen. At zero magnetic field the acoustic wave will be launched from the generating surface with its polarization parallel to the induced current direction. When the sound wave reaches the detector coil, it is clear that the maximum signal is induced if the coil winding directions are parallel. At high magnetic field the polarization of the sound wave is nearly perpendicular to the generating-coil windings. But at the opposite surface of the metal sample the maximum signal is once again recovered when the detector-coil winding direction is nearly perpendicular to the polarization of the sound wave, by symmetry, or parallel to the generating-coil windings. In the intermediate field region an argument resolving the signal into components gives the same result. So one can see that while the coil-coil measurement eliminates transducer problems, only one quantity instead of two can be determined.

In fitting the theory curve for the generation amplitude to the data we have assumed that the high-field behavior is consistent with local theory. This fact has been well verified in aluminum by Gaerttner.[9] Let us define two ratios:

$$R_{\text{expt}} = (\xi_H/\xi_E)_{\text{expt}}\,,$$
$$R_{\text{theor}} = (\xi_H/\xi_E)_{\text{theor}}\,, \tag{8}$$

where expt and theor stand for experimental and theoretical. For simplicity ξ_H represents $|\vec{\xi}_H|$; likewise for ξ_E. Using the experimental result that the high-field theory agrees with the high-field data gives

$$(\xi_H)_{\text{expt}} = (\xi_H)_{\text{theor}}\,, \tag{9}$$

and therefore,

$$(\xi_E)_{\text{expt}}/(\xi_E)_{\text{theor}} = R_{\text{theor}}/R_{\text{expt}}\,, \tag{10}$$

where R_{theor} depends only on ql. R_{expt} is determined from the data, and R_{theor} is easily calculated from Eqs. (3)–(6). The value of the sound velocity s in Eq. (2) is determined from the measured

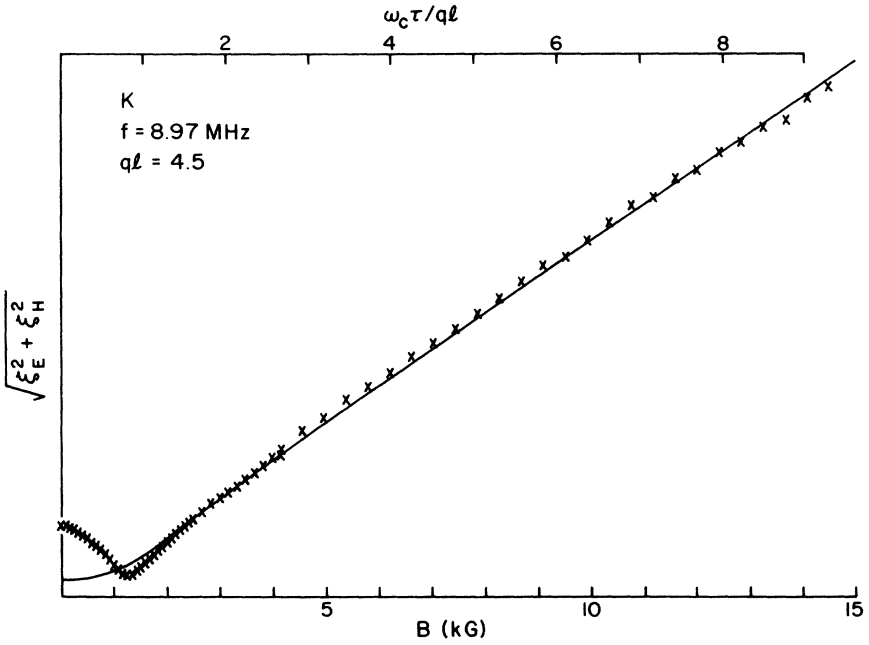

FIG. 4. Electromagnetic generation amplitude vs magnetic field at $T = 4.2$ K. Vertical scale is in relative units. Solid curve is theory for $ql = 4.5$, normalized at high field.

elastic constants of potassium,[18] and for Fermi-surface parameters, free-electron values have been used.

V. RESULTS AND DISCUSSION

The principal results of this experiment are presented in Figs. 4–6. Figure 4 shows the magnetic field dependence of $(\xi_E^2 + \xi_H^2)^{1/2}$ from 0 to 15 kG. The data points are representative values from the continuously monitored signal amplitude. For comparison, the solid theory curve for $ql = 4.5$ is also displayed. The high-field values of the data are normalized to theory, as described in Sec. IV. Note the excellent agreement above about 5 kG. It should be remembered that the data plotted in Fig. 4 represent the square root of the experimental signal, so the linearity of $(\xi_E^2 + \xi_H^2)^{1/2}$ from 5 to 15 kG provides an additional check on our method. At low magnetic fields, however, we see that agreement with theory is not obtained.

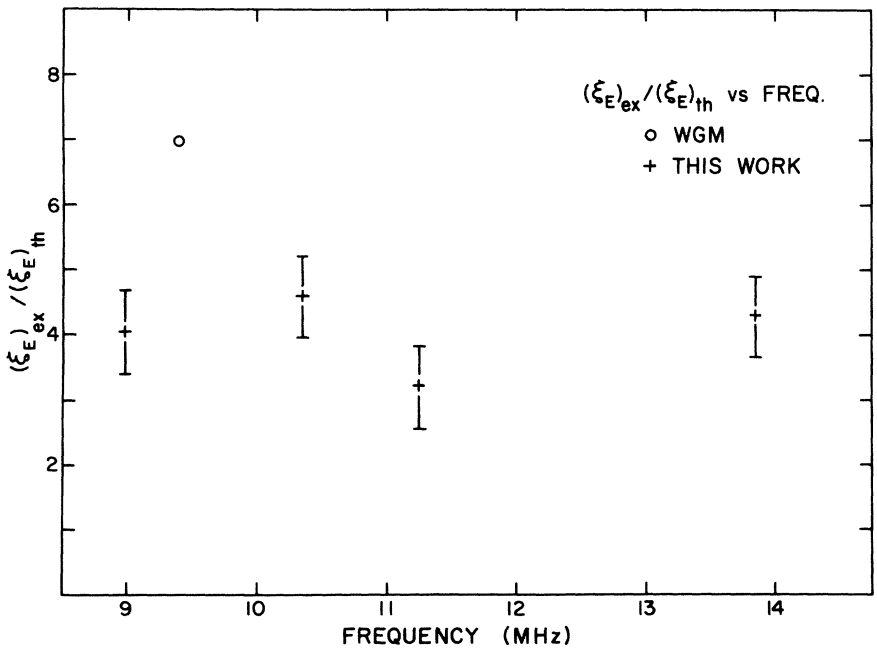

FIG. 5. Ratio of measured to theoretical electromagnetic generation amplitude at zero field vs frequency. WGM is Ref. 8.

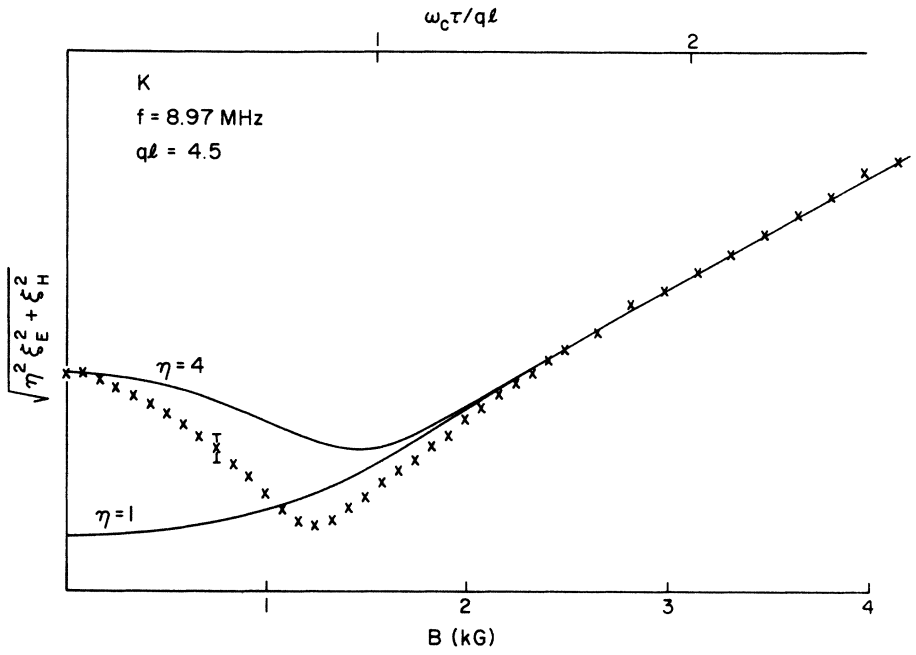

FIG. 6. Electromagnetic generation amplitude vs magnetic field. Solid curves are theory for $ql = 4.5$. In upper curve ξ_E is arbitrarily normalized to data at zero field as explained in text.

The zero-field amplitude is about four times larger than predicted by theory. As well, there is a monotonic decrease in the signal to a minimum at about 1 kG, at which point the amplitude is below the theory curve. This disparity at zero field is in qualitative agreement with WGM.[8] They find that $(\xi_E)_{expt}/(\xi_E)_{theor}$ is about 7 in a sample where $ql = 2$.

It is clear from Fig. 1 that no value of ql can bring the theory into agreement with the data at zero field.[19] This major result of our experiment contradicts the work of TTH, who find good agreement with free-electron theory at 30 and 50 MHz. Although our apparatus could not reach these high frequencies, we did measure ξ_E at frequencies ranging from 9 to 14 MHz. Figure 5 shows the ratio $(\xi_E)_{expt}/(\xi_E)_{theor}$ plotted versus frequency. For completeness, we have included the measurement of WGM. Since it is possible to draw a horizontal line through our experimental points, we conclude that the disagreement with theory is largely independent of frequency.

A further attempt to obtain agreement between our results and free-electron theory by scaling the zero-field prediction is presented in Fig. 6. Here, the experimental points are plotted from 0 to 4 kG as in Fig. 1, along with the theory curve for $ql = 4.5$. In addition to these, we have also displayed a curve derived from theory which represents the expression $(\eta^2\xi_E^2 + \xi_H^2)^{1/2}$, where η is an arbitrary scaling factor that has been chosen to force agreement with the data at zero field. However, even with this extreme and unphysical assumption, it is still impossible to produce substaintial agreement with theory. Detailed comparison with TTH in the low-field region is difficult because they report no results for ξ_H between 0 and 1 kG.

We stated earlier that the present experiments have been undertaken in order to resolve the disparity between WGM and TTH. Because of the strong disagreement with free-electron theory in potassium, the results of WGM were initially viewed with some skepticism. And although the previous work by WGM was performed in this laboratory, the current experiment makes use of different samples and different experimental techniques, including almost all of the experimental apparatus. However, since the present results are so similar in many respects to the earlier data, we have carried out a systematic review of the free-electron calculations.

It is believed that the local free-electron theory correctly describes the high-field result and thus determines accurately the constant A in Eq. (6). For the zero-field prediction one could view the electron mean free path as a parameter to be determined by the best fit to experiment. Yet Fig. 1 shows that there is no value of l that produces good agreement with the data. What is most disconcerting is that the experimental amplitude at zero field is considerably *larger* than the theoretical prediction. One can think of many reasons why the measured amplitude might be smaller than the theoretical value, but it is difficult to do the opposite. Nonetheless, the following several arguments attempt to demonstrate how the theory might be modified to give a larger prediction for the zero-field EG amplitude.

Consider the nonmagnetic component at zero magnetic field. The generation amplitude is the sum of two competing forces. The electric field in the skin depth acts on the ions causing them to accelerate. The electric field also accelerates the conduction electrons and they collide with the lattice, providing an additional but opposite force. In the local limit these two forces exactly cancel, so there is no net effect. In the case of nonlocal conduction complete (microscopic) cancellation no longer occurs, and nonmagnetic generation is observed. Since there is this competition between forces, one is led to treat the forces separately.

Consider the electron reaction force $\vec{F}_r$ of Eq. (1) to be multiplied by a coefficient α. For $\alpha = 1$ we recover the free-electron result, and for $\alpha = 0$ the reaction force is ignored altogether, thus obtaining a maximum amplitude. Under this postulate the nonmagnetic generation amplitude becomes

$$\vec{\xi}(z=0) = (2A/\omega\tau)\hat{x}\,\mathrm{Re}(\alpha - G_{+}^{-1}) . \qquad (11)$$

In Fig. 7 we plot the ratio of $\xi(\alpha)/\xi(\alpha=1)$ as a function of ql for $B=0$. This expression gives the enhancement of the nonmagnetic component for various values of α. Clearly, the high-field amplitude is independent of α. For $ql \approx 4$, even ignoring the reaction altogether will not increase the zero-field result more than 70%, whereas a factor of 4 is needed to produce agreement with experiment. Therefore we can conclude that the reaction force does not influence the EG amplitude substantially in the region where $ql \gtrsim 1$.

As a further critical review of the theory, the assumption of specular scattering of electrons at the surface has been examined. In a series of careful calculations, Stevenson[20] has found that near 10 MHz the zero-field generation for the case of purely diffuse scattering or any combination of diffuse and specular scattering is enhanced by no more than 15% over the specular result and that the high-field magnetic component does not depend on surface scattering. Although this modification takes the theoretical result in the right direction, once again it is clearly insufficient to explain the disparity.

The surface region of a metal may sometimes have properties different from the bulk owing to impurities, vacancies, or dislocations near the surface. One can estimate the effect of having electronic characteristics in the surface region which are different from the bulk material. The nonmagnetic EG amplitude depends on the electron mean free path near the surface, while the high-field magnetic component is unaffected by l as long as $\omega\tau \ll 1$. If l_{surface} were significantly smaller than l_{bulk}, the measured ratio ξ_E/ξ_H would be smaller than ξ_E/ξ_H calculated for l_{bulk}, although this apparent disparity becomes less pronounced as ql increases. It is possible that the etching procedure followed by TTH after attaching a transducer to the same surface used to detect or generate the EG amplitude did not completely remove damage in the surface region of their specimen. Although these procedures might lead to a surface electrically different from the bulk, we have calculated that a reduction from $ql = 10$ to $ql = 1$ at constant frequency would decrease ξ_E by only a factor of 2.5, insufficient to account for the difference between their data and ours. Another possible problem is that the transducer measurement of attenuation used to correct the EG data was obtained in a different run. If the attenuation was affected by the intervening transducer mounting, this circumstance might lead to errors in the field-dependent extrapolation. Admittedly, any systematic error which resulted in close agreement with the free-electron value of ξ_E/ξ_H at three frequencies is rather unlikely.

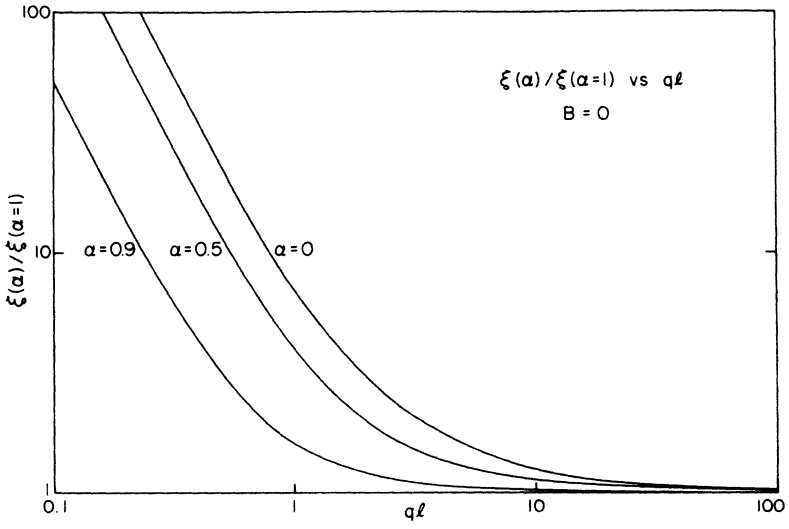

FIG. 7. Enhancement of electromagnetic generation amplitude vs ql. α is a weighting factor for the electron reaction force.

Finally, one might suggest that the surface of the sample is coated with oxide. If the oxide layer is strongly bound to the surface, the appropriate boundary condition would be closer to that for a fixed surface, $\vec{\xi}(z=0)=0$. Calculations show that a fixed surface reduces both the magnetic and nonmagnetic components by a factor of the order of $q\delta \approx 10^{-2}$ for our experimental parameters. Signals this small would be experimentally undetectable at zero field.

In conclusion, our experiment has sought to relieve the ambiguity in previous work by providing a measurement of EG amplitude as a function of magnetic field without the complication of piezoelectric transducers. Instead of achieving close agreement with free-electron theory, these new, more general results display much the same disturbing features observed by Wallace, Gaerttner, and Maxfield.[8] While we readily admit that both the measured magnitude and field dependence of the acoustic attenuation are still troublesome features of our results, we believe that spurious effects cannot account for our data. The monotonic decrease of the signal from 0 to 1.3 kG is not at all reproduced by theory and is present even in the raw data uncorrected for attenuation. We have found that the zero-field EG amplitude is several times larger than the free-electron prediction, and the low-field behavior of $\vec{\xi}$ is suggestive of the previously measured anomaly.[8] In addition, every reasonable attempt to modify the theory to make it consistent with the data has fallen short of success. Perhaps there exists a yet undiscovered modification of the theory that will produce agreement with experiment. For now, it seems reasonable to withhold judgment and suggest that further experimental verification might be needed. In particular, since TTH observe good agreement between theory and experiment at higher frequencies (~30 MHz), it would be useful to extend the coil-coil measurements to this frequency regime. Also, a comparison of coil-coil and coil-quartz or single-ended quartz attenuation measurements might expose a subtle problem with the coil-coil attenuation data.

Note added in proof. The theoretical work of E. A. Kaner and V. L. Fal'ko {Zh. Eksp. Teor. Fiz 64, 761 (1973) [Sov. Phys.-JETP 37, 516 (1973)]} has just appeared in translation and claims to obtain an exact solution of the electromagnetic generation problem which agrees with experiment. They include a deformation potential which reflects distortions of the Fermi surface by the acoustic wave. We do not fully understand their complicated analysis, but we have examined their final results. The zero-field amplitude ξ_E they obtain is larger than ours by about a factor of 3 and is closer to our experimental value. Their ξ_E however does not go to zero at high fields but instead approaches about $\frac{1}{2}$ of its zero field value. This does not agree with the experiments of TTH or WGM. Although not directly related to the present work, their analysis does produce the nonmonotonic behavior of ξ_H observed by WGM, but their theory requires ql to be 10 in order to show the effect, whereas WGM estimated ql to be about 2.

ACKNOWLEDGMENTS

The authors are pleased to acknowledge David J. Stevenson for many helpful discussions and John W. Wilkins for a critical reading of the manuscript.

*Work supported mainly by the U.S. Atomic Energy Commission under Contract No. AT(11-1)3150. Additional support was received from the Advanced Research Projects Agency and the National Science Foundation, Grant No. GH-33637, through the use of the technical facilities of the Cornell Materials Science Center.

[1]P. K. Larsen and K. Saermark, Phys. Lett. A 24, 374 (1967).

[2]J. R. Houck, H. V. Bohm, B. W. Maxfield, and J. W. Wilkins, Phys. Rev. Lett. 19, 224 (1967).

[3]W. D. Wallace, M. R. Gaerttner, and B. W. Maxfield, Bull. Am. Phys. Soc. 14, 64 (1969).

[4]M. R. Gaerttner, W. D. Wallace, and B. W. Maxfield, Phys. Rev. 184, 702 (1969).

[5]R. L. Thomas, G. Turner, and D. Hsu, Phys. Lett. A 30, 316 (1969).

[6]J. J. Quinn, Phys. Lett. A 25, 522 (1967).

[7]G. Turner, R. L. Thomas, and D. Hsu, Phys. Rev. B 3, 3097 (1971).

[8]W. D. Wallace, M. R. Gaerttner, and B. W. Maxfield, Phys. Rev. Lett. 27, 995 (1971).

[9]M. R. Gaerttner, Ph.D. thesis (Cornell University, 1971) (unpublished).

[10]R. C. Alig, Phys. Rev. 178, 1050 (1969).

[11]T. Kjeldaas, Phys. Rev. 113, 1473 (1959).

[12]D. E. Chimenti and B. W. Maxfield, Phys. Rev. B 7, 3501 (1973).

[13]Supplied by MSA Research Corp., Evans City, Pa.

[14]For a complete study of the effects of isothermal cooling on potassium, see J. W. Ekin, Ph.D. thesis (Cornell University, 1971) (unpublished).

[15]T. G. Blaney, Philos. Mag. 17, 405 (1968).

[16]A. B. Pippard, Philos. Mag. 2, 1147 (1957).

[17]Giovan G. Natale and Isadore Rudnick, Phys. Rev. 167, 687 (1968).

[18]W. R. Marquardt and J. Trivisonno, J. Phys. Chem. Solids 26, 273 (1965).

[19]The fact that the curves for $ql \gg 1$ and $ql \ll 1$ cross at low field is explained by noting that the nonlocal magnetic component, while linear at low fields, has a smaller slope than the local magnetic component when $\omega_c < qv_F$. Since the nonmagnetic component is important only in the nonlocal case, the quantity $(\xi_E^2+\xi_H^2)^{1/2}$ will be larger at zero field for the nonlocal case and a smaller than the local result at some intermediate field near $\omega_c = qv_F$. A full discussion of nonlocal magnetic generation is presented in Ref. 9.

[20]D. J. Stevenson, (private communication).